

MICROSCOPIC TIME-REVERSIBILITY AND MACROSCOPIC IRREVERSIBILITY — STILL A PARADOX?

Harald A. Posch,¹ Christoph Dellago,¹ William G. Hoover,² and
Oyeon Kum²

¹Institute for Experimental Physics
University of Vienna
Austria

²Department of Physics
Lawrence Livermore National Laboratory
and Department of Applied Science
University of California at Davis/Livermore
Livermore, CA

Microscopic time reversibility and macroscopic irreversibility are a paradoxical combination. This was first observed by J. Loschmidt in 1876 and was explained, for conservative systems, by L. Boltzmann the following year. Both these features are also present in modern simulations of classic many-body systems in steady nonequilibrium states. We illustrate them here for the simplest possible models, a continuous one-dimensional model of field-driven diffusion, the so-called driven Lorentz gas or Galton Board, and an ergodic time-reversible dissipative map.

1. INTRODUCTION

In classical statistical mechanics, Loschmidt and Zermelo are notorious for their criticism of Boltzmann's explanation of irreversibility. For isolated systems far from equilibrium Boltzmann predicted a unidirectional irreversible decay toward mechanical and thermal equilibrium. This prediction was based on his H-Theorem description of gas-phase entropy production¹ and is an exact consequence of the Boltzmann Equation for the time development of the one-particle distribution function $f(\mathbf{r}, \mathbf{v}, t)$. The approximation underlying this equation is the *Stosszahlansatz* which is a replacement of the two-particle collisional probability by a product

of one-particle distributions. The Boltzmann equation predicts a monotone decrease of $\langle \ln f \rangle$ following the time evolution of the system, and the Boltzmann entropy

$$S(t) = -k \langle \ln f \rangle = -k \int f(\mathbf{r}, \mathbf{v}, t) \ln f(\mathbf{r}, \mathbf{v}, t) d\mathbf{r} d\mathbf{v} \quad (1)$$

in the limit $t \rightarrow \infty$ approaches the Gibbs entropy per particle.^{5,6} k is the Boltzmann constant.

Loschmidt objected that this predicted irreversibility is inconsistent with the underlying time-reversible equations of motion, because any trajectory going *toward* equilibrium could just as well be followed in the reversed direction, *away* from equilibrium.² Zermelo insisted that the irreversibility is likewise inconsistent with Poincaré's theorem, which states that the phase trajectory of an isolated mechanical system will eventually revisit a small neighborhood of its initial phase point.³ Both objections certainly seem valid. However, as Boltzmann immediately pointed out,⁴ any argument based on a phase trajectory linking nonequilibrium states with equilibrium states needs to consider not only the time-reversible nature of the equations of motion but also the probability distribution of the initial conditions. In the case of Loschmidt's objection this probability for a macroscopic system is so much in favor of the equilibrium states that any dynamical evolution or even fluctuation leading from equilibrium to nonequilibrium states is practically unobservable. It also makes Poincaré's recurrence time ridiculously long. It is easy to imagine that Boltzmann's approximate statistical treatment of two-body collisions is responsible for the apparent contradictions. Though designed to describe systems obeying reversible dynamical laws, the approximation makes the Boltzmann equation intrinsically irreversible. As a consequence, it fails to describe some phenomena, primarily phenomena involving fluctuations.

In the present work we do not intend to treat equilibration of isolated systems. This is discussed in depth in the article by H. Spohn in this volume. We prefer instead to attempt a better understanding of explicitly *nonequilibrium* systems, systems driven away from equilibrium by boundary conditions which impose velocity or temperature gradients on them and impose a steady nonequilibrium state. For such systems, free to undergo corresponding *reversible* momentum and energy exchanges with their surroundings, it is no longer true that all phase-space states are equally likely.

Nevertheless, the motion is — in a certain sense (which will be clearly defined for our two models) — “ergodic” so that Zermelo's objection applies with full force. Any observed state, including the initial state, will eventually recur. Also, Loschmidt's objection still holds when time-reversible equations are used to describe the interactions with the surroundings. Any system evolving in accord with the Second Law of Thermodynamics becomes a system violating that Law when time is reversed. In the present work we restrict consideration to ergodic time-reversible systems and show that, despite the ergodicity and despite the time-reversibility, the motion — averaged over a long trajectory — *is* dissipative and irreversible, and the phase-space distribution for steady nonequilibrium states collapses to a strange attractor. We believe that the two simple models which exhibit all this complexity and are discussed in the following two Sections are instructive aids to understanding the irreversibility described by the Second Law.

The time-reversible equations of motion for a particle which we shall use in the following have the general form

$$\dot{\mathbf{q}}_i = \mathbf{p}_i/m, \quad (2)$$

$$\dot{\mathbf{p}}_i = \mathbf{F}_i(\mathbf{q}) + \mathbf{X}_i + \mathbf{F}_i^C(\mathbf{q}, \mathbf{p}), \quad (3)$$

where $\mathbf{q}_i, \mathbf{p}_i$ are the position and momentum vectors of particle i . For simplicity, all the particles have equal mass m . The arguments \mathbf{q} and \mathbf{p} without index i stand for the positions and momenta of all particles. In this equation $\mathbf{F}_i(\mathbf{q}) = -\partial\Phi(\mathbf{q})/\partial\mathbf{q}_i$ is the intrinsic force on particle i , where $\Phi(\mathbf{q})$ is the potential energy, and \mathbf{X}_i is an external force driving the system away from equilibrium. Through \mathbf{X}_i work is continuously performed, which — if not properly taken care of — would heat or cool the system and prevent a steady state. This is conveniently avoided by the constraint force

$$\mathbf{F}_i^C(\mathbf{q}, \mathbf{p}) = -\zeta\mathbf{p}_i \tag{4}$$

describing the action of a heat reservoir, where $\zeta(\mathbf{q}, \mathbf{p})$ is a dynamical variable which changes sign with time reversal and is referred to as a thermostat or friction variable. The particularly simple and aesthetic form of a time-reversible constraint force in (4) is a consequence of venerable variational principles of mechanics, including both Hamilton’s *Principle of Least Action*⁷ and Gauss’ *Principle of Least Constraint*.^{8–10} For such a description to agree with macroscopic thermodynamics it is specially useful to define temperature in terms of the ideal-gas thermometer, $kT \equiv \langle p_\alpha^2/m \rangle$, where p_α is the momentum of a typical cartesian degree of freedom.

Once this idea of a time-reversible nonequilibrium steady-state system with a constraint force (4) is accepted, a number of consequences follow directly from the equations of motion^{10–12}

1. The equations of motion, both at and away from equilibrium, remain exactly time-reversible, so that a reversed movie of the motion obeys the same equations. In such a reversed motion all the momenta \mathbf{p}_i and the thermostat variable ζ change sign. There are other concepts of a time-reversible system which differ from that used in this paper. We shall come back to this point in Section 4. For simplicity we have assumed that all N particles in the physical space of dimension d are constrained to a single boundary temperature T requiring a single thermostat variable ζ . But these ideas may be generalized to more than one friction variable controlling different degrees of freedom.
2. There is a *nonequilibrium* version of Liouville’s Theorem, which identifies the rate of heat loss, $-\sum_{i=1}^N \zeta\mathbf{p}_i^2/m$, divided by the corresponding boundary temperature T and Boltzmann’s constant k , with the rate of shrinkage of an arbitrary (differentially small) comoving phase-space volume element δV :

$$d \ln \delta V / dt = - \sum_{i=1}^N \zeta \mathbf{p}_i^2 / mkT = -Nd\zeta = (dQ/dt)/kT. \tag{5}$$

3. Since the exponential growth or shrinkage of (infinitesimally small) phase-space perturbations of the system’s trajectory are measured in terms of the Lyapunov exponents λ_l , the time-averaged shrinkage of a comoving phase-space volume element is given by the sum of all Lyapunov exponents:

$$\langle d \ln \delta V / dt \rangle = \sum_{l=1}^L \lambda_l \leq 0, \tag{6}$$

where $L = 2dN$ is the dimension of the phase space. The equal sign applies only for equilibrium systems. In nonequilibrium steady states with a steady external boundary temperature T , the exchanges of heat lead to the $<$ sign in (6) indicating the collapse

of the corresponding phase-space probability into a strange attractor with a fractional dimension D_1 . This so-called information dimension D_1 can be thought of in two distinct ways: first, as the way in which the phase-space probability within a hyperbox of size ε depends upon ε , namely $\sim \varepsilon^{D_1}$, averaged over a whole partition of the phase space with such boxes; second, as the dimensionality of a phase space object whose phase-space measure — on the average — neither grows, nor shrinks, as time progresses. At equilibrium the information dimension is identical to the dimension D_0 of the allowed phase space. Away from equilibrium this dimensionality is reduced, $D_1 < D_0$, though the motion itself, if ergodic, continues to visit — eventually — all points of the equilibrium phase space. Thus, the *full* equilibrium phase space is required to support the measure in the nonequilibrium steady state, and D_0 is equal to the Hausdorff dimension, the dimension of the support of the measure.¹³

4. The time reversibility of the motion equations guarantees, in addition to the strange attractor, also an exactly similar strange repellor, which is constructed from the attractor points by reversing the sign of all momentum components and thermostat variables. Its support is again the full equilibrium phase space, and it is likewise ergodic.
5. The repellor acts as a “source” of the space flow in the same way that the attractor acts as a “sink.” The Lyapunov-unstable ($\sum \lambda > 0$) repellor states (occupied in the distant past) are connected to the Lyapunov-stable ($\sum \lambda < 0$) attractor states (to be occupied in the distant future) by ergodic trajectories in phase space which come arbitrarily close to every point of the (allowed) equilibrium phase space. A time-reversal transformation transforms stable attractors into unstable repellors and *vice versa*.

In the present work we discuss two examples which exhibit all these puzzling features. The first is the externally driven Lorentz Gas or Galton Board. Both the ergodicity, the fractal nature of the phase-space distribution and the reduction of the information dimension have been established rigorously,^{14,15} confirming earlier numerical work.^{16,17} Recently we have developed an exact algorithm for the computation of Lyapunov spectra of particle systems involving hard elastic collisions, which has been applied also to this model.^{19,20} The second example is a class of simple time-reversible two-dimensional maps which exhibit exactly the same features — reduced information dimension with ergodic attractor-repellor pairs — but with reduced complexity.²¹ Both examples exhibit irreversible behavior, and both are subject to Loschmidt’s and Zermelo’s objections. We present these two models in Sections 2 and 3 and discuss the results in Section 4.

2. EXTERNALLY DRIVEN PERIODIC LORENTZ GAS OR GALTON BOARD

The simplest model for nonequilibrium transport is that of a point mass, referred to as the wanderer particle, driven through an infinite periodic lattice of elastic hard scatterers by an external field. In the two-dimensional case we consider here the scatterers are hard disks arranged in a triangular lattice as shown in Figure 1. Due to the collisions with the scatterers the wanderer performs a diffusive motion in the corresponding field-free case for which the mean squared displacement approaches $2Dt$ at long times t , where D is the diffusion coefficient.²²

The wanderer motion could equivalently be viewed more symmetrically, as relative motion in a periodic *two-body* system, with vanishing center-of-mass velocity. However, here

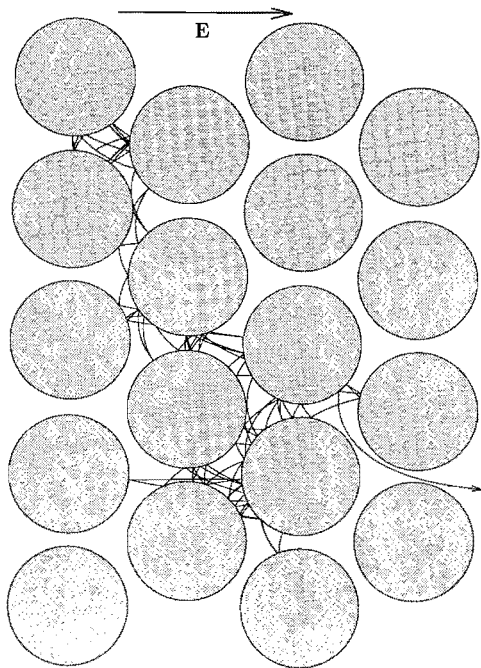


Figure 1. Geometry of the externally driven periodic Lorentz Gas also referred to as the Galton Board. E is an external field which drives a point particle of mass m through an infinite periodic triangular lattice. The scatterer density is $4/5$ of the close-packed density. A single trajectory is shown.

we will adopt the view that a single particle, with mass m , moves through a lattice of fixed scatterers. With periodic boundaries and a symmetric direction of the field E the motion can be restricted to one half of a single unit cell.

Numerical investigation has shown that the motion, periodically confined to a single half unit cell, is ergodic for sufficiently small fields, just as it is in the zero-field case.^{16,17} This result was also established theoretically.¹⁵ We describe it with Boltzmann's term "ergodic," meaning that the moving particle eventually, and repeatedly, comes arbitrarily close to any point $\{x, y, p_x, p_y\}$ of the allowed phase space. For a fixed scatterer density the only available control parameters are the kinetic energy $\mathbf{p}^2/2m$ and the driving field strength $E = |\mathbf{E}|$. Then the shape of the wanderer trajectory only depends on the dimensionless ratio EmR/\mathbf{p}^2 , which determines the influence of the field energy relative to the kinetic energy. R is the radius of the scatterer (see Figure 2).

During the streaming between successive collisions the wanderer is accelerated by the field. To achieve a *stationary nonequilibrium state* it is convenient to constrain the kinetic energy, using the linear constraint force (4). If the field points in x -direction the equations of motion suggested by Hamilton's and Gauss' principle become

$$\begin{aligned} \dot{x} &= p_x/m & ; & \dot{y} = p_y/m \\ \dot{p}_x &= E - \zeta p_x & ; & \dot{p}_y = -\zeta p_y, \end{aligned} \quad (7)$$

where the thermostat variable assumes the form

$$\zeta = p_x E / \mathbf{p}^2. \quad (8)$$

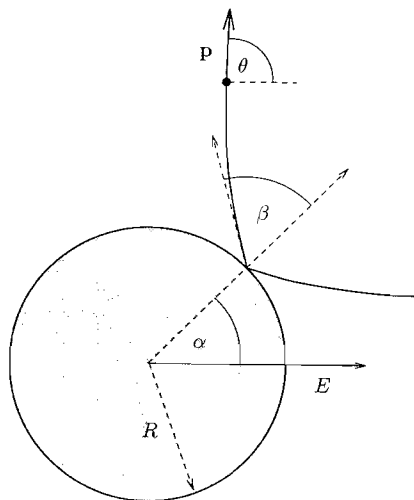


Figure 2. Geometry of a collision between the wanderer and a scatterer particle.

The wanderer dynamics in Figure 1 takes place in a three-dimensional phase space $\{x, y, \theta\}$, where θ defines the direction of the particle with respect to the field as shown in Figure 2:

$$p_x = p \cos \theta; p_y = p \sin \theta. \quad (9)$$

As a further simplification we observe the state of the wanderer particle only *at* its collision with the scatterer, ignoring the smooth streaming between collisions. This corresponds to the construction of a Poincaré map and reduces the three-dimensional description to a two-dimensional map in collision space $\{\alpha, \sin \beta\}$, where the collisional angles α and β are also defined in Figure 2. $\sin \beta$ changes sign during time reversal and is thus a momentum-like variable, whereas α is a position variable describing the collision.

In the field-free equilibrium case all collisions in the $\alpha, \sin \beta$ -plane are equally likely as shown in Figure 3a. In this example the scatterer density is $4/5$ the close-packed value. The nonequilibrium set of collision points in Figure 3b for a rather weak field, $EmR/p^2 = 1.5$, and in Figure 3c for the moderately strong field, $EmR/p^2 = 3.0$, reveal a multifractal structure, which we referred to as a strange attractor in the Introduction. The singularity strength a of the probability density varies from point to point. a determines how the measure μ_ε of a neighborhood of a point scales with the size ε of this neighborhood, $\mu_\varepsilon \sim \varepsilon^a$. The phase-space distribution is singular almost everywhere.

The multifractal nature of this distribution can be characterized by the singularity spectrum $f(a)$, which, loosely speaking, is the Hausdorff (box counting) dimension of the set of all points characterized by a local singularity strength a .²³ The curve A in Figure 4 was obtained with a box-counting algorithm due to Chhabra and Jensen²⁴ and depicts the singularity spectrum for the attractor in Figure 3b. The various symbols refer to different box sizes; up to 1024×1024 boxes were used. The spectrum is reliable for $a < 2.5$, which is the range of interest for our purposes. Vance has shown that the descending and ascending parts of the spectrum are simply related,¹⁵

$$(a-1)f\left(\frac{a}{a-1}\right) = f(a) + a - 2. \quad (10)$$

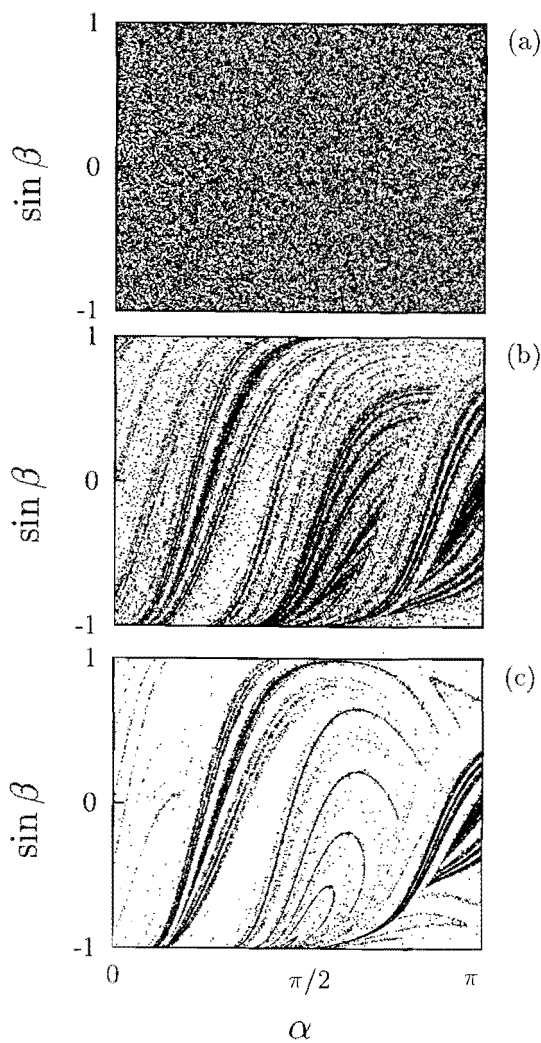


Figure 3. Poincaré map in the collisional $\alpha, \sin\beta$ -plane for the driven Lorentz Gas (Galton Board) model. 50,000 collision points are shown in each plot. (a) field-free case, $E = 0$; (b) $EmR/p^2 = 1.5$; (c) $EmR/p^2 = 3.0$. The scatterer density is $4/5$ of the close-packed density.

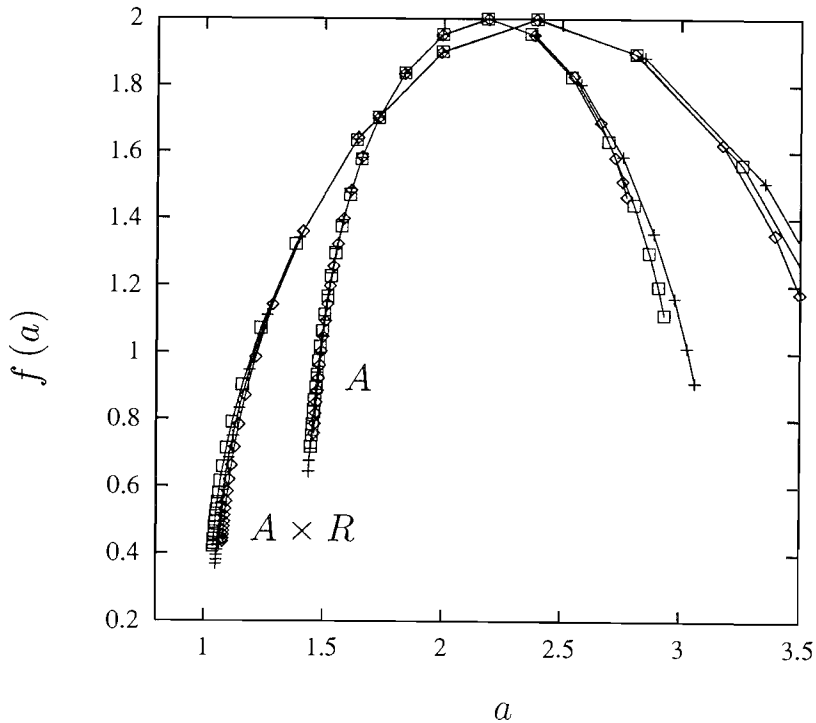


Figure 4. Singularity spectrum, $f(a)$, for the driven Lorentz Gas (Galton Board) model. The scatterer density is $4/5$ of the close-packed density, the field is $EmR/p^2 = 1.5$. Curve A: $f(a)$ for the attractor depicted in Figure 3b; Curve A \times R: $f(a)$ for the attractor-repellor product measure defined in equation (12).

This relation is well obeyed by spectrum A for the fractal object depicted in Figure 3b. The information dimension is equal to that value of the singularity spectrum for which $f(a) = a$ or, equivalently, $f'(a) = 1$. D_1 is also referred to as the Hausdorff dimension of the set of the probability measure,²⁵ but should not be confused with D_0 , the Hausdorff dimension of the support of that measure. D_0 , is given by the maximum of the $f(a)$ -curve. For our example $D_1 = 1.82$, and $D_0 = 2 > D_1$ in agreement with our previous assertion.

The information dimension D_1 of the multifractal is also related to the conductivity $\kappa = \langle p_x/mE \rangle$ and to the Lyapunov spectrum of the system.^{9, 10, 26} Vance found that the change in information dimension due to the field is given by¹⁵

$$\Delta D_1 = \kappa E^2 m / (p^2 \lambda_{min}), \quad (11)$$

where λ_{min} is the most negative Lyapunov exponent. A similar result, identical through terms quadratic in the field strength E , was subsequently obtained by Chernov, Eyink, Lebowitz and Sinai.^{14, 18}

Until recently accurate Lyapunov exponents were not available for the Lorentz Gas. We have developed a method which is based on following differentially-separated trajectories in tangent space and which takes the impulsive hard-disk collisions exactly into account.^{19, 20} It is valid at arbitrary high fields. The theoretical prediction (11) is verified by our computer-simulation results. For instance, if we consult Table 1 of Ref. 19 referring to a scatterer density of $4/5$ of its close-packed value, we find: $\kappa = 0.146$, $E = 1.50$, $\lambda_{min} = -1.829$, and $\Delta D_{KY} = -0.180$. These quantities are given here in reduced units for which p, m , and R are

all unity, and D_{KY} is a dimension derived from the Lyapunov spectrum and — according to the Kaplan-Yorke conjecture — is expected to be equal to the information dimension D_I . The expression (11) yields for the dimensionality reduction $\Delta D_I = -0.18$ in perfect agreement with our direct computation. Since both numbers are the results of independent measurements, we conclude that our present understanding of the driven Lorentz Gas, from a numerical standpoint, is quite satisfactory.

This is not the case for our theoretical understanding. The paradoxical features of the phase flow, identified by Loschmidt and Zermélo, still remain, namely its time reversibility and ergodicity. Going forward *or* backward in time eventually leads to shrinkage in the phase space, although the reversal of any particular step simply changes the sign of the rate with which the phase volume changes. Starting at $t = 0$ from almost any point in phase space and going forward in time, the system trajectory generates a stable strange attractor with a negative Lyapunov-exponent sum. If at time $t = \tau \gg 0$ the system is in a state $\{\mathbf{r}(\tau), \mathbf{p}(\tau)\}$ on or close to this attractor, a time reversal transformation gives a state $\{\mathbf{r}(\tau), -\mathbf{p}(\tau)\}$ on or close to the strange repeller. The reversed trajectory — although a valid solution of the time-reversible equations of motion — is now characterized by a positive sum of Lyapunov exponents and is more unstable than the forward trajectory: Macroscopic time reversibility is broken. If we continue to follow the reversed trajectory for times $t > \tau$ it will therefore leave the repeller states and - at a time 3τ — will be close or on the attractor again. Theoretically the limit $\tau \rightarrow \infty$ is understood. For all practical applications, a few Lyapunov times are sufficient. In the case detailed above the attractor and repeller dimensions are 1.82, a drop of $\Delta D_I = -0.18$ from the equilibrium value.

Vance observed that these fractal objects are ergodic.¹⁵ Intuitively this is to be expected on the basis of the reversibility of the equations of motion. Any zero-measure portion of the attractor must correspond to zero measure in all other portions of the attractor connected to the original portion by the phase flow. Because the attractor and repeller are ergodic, in any arbitrarily small neighborhood of each attractor point there will be repeller points and *vice versa*. For our weak-field example of Figure 3b this is depicted in Figure 5, in which attractor and repeller points are superimposed.

We have tried to analyze this complicated topological structure by evaluating the multifractal singularity spectrum for the correlation measure μ_{AR} defined in terms of the numbers of attractor and repeller points, N_A and N_R , for all boxes of a partition of the Poincaré map with box size ε :

$$\mu_{AR} \equiv N_A N_R / \sum N_A N_R. \quad (12)$$

Here, the sum is over all boxes. In Figure 4 the singularity spectrum for the attractor-repeller product measure (label $A \times R$) is compared to that of the pure attractor (label A). The various symbols refer to different box sizes. The Hausdorff dimension of this product measure, given by the maximum of the $f(a)$ -curve, equals two as expected. Its information dimension is 1.64, less than that of the pure attractor. As may be seen from Figure 4, the multifractality of the product measure is greatly enhanced.

We have mentioned already that infinitesimally close to every attractor point lie repeller points and *vice versa*. There is, however, no obvious spatial correlation between a point on the attractor with its repelling neighbors. This is demonstrated in Figure 6 where we plot generalized correlation integrals $C(r)$ obtained from the Poincaré map of Figure 3b. Such integrals were used by Grassberger and Procaccia²⁷ for the evaluation of the correlation dimension D_2 . Let us consider two sets of points, S_1 and S_2 , each containing M points in the same space. Then $C(r)$ is defined as the number of points belonging to S_2 and which have

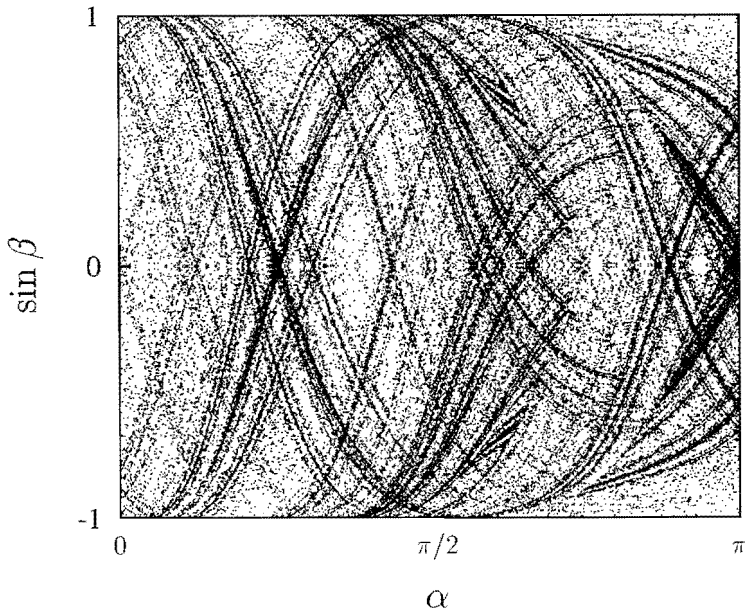


Figure 5. Superposition of the maps representing the strange attractor and strange repeller for the driven Lorentz Gas (Galton Board) model for a field $EmR/p^2 = 1.5$. The scatterer density is $4/5$ of the close-packed density.

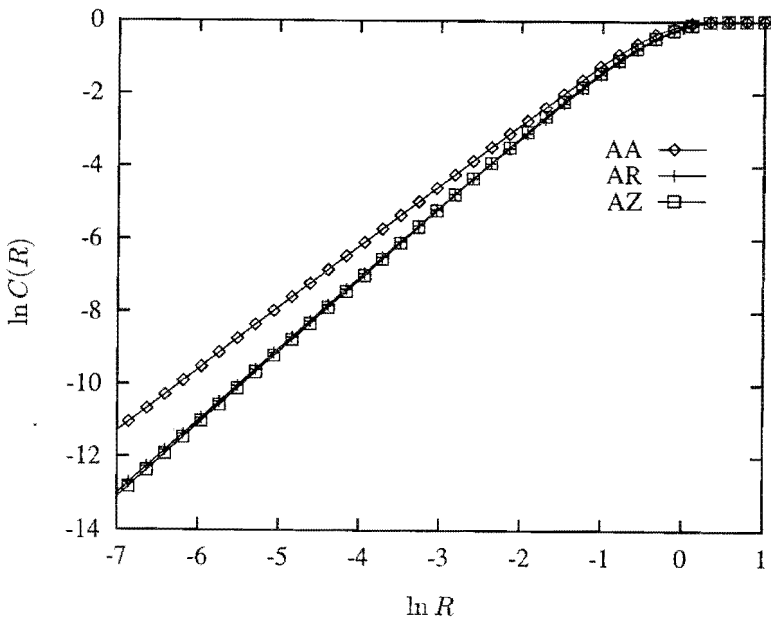


Figure 6. Generalized correlation integrals $C(r)$ for the driven Lorentz Gas (Galton Board) as defined in Section 2. The scatterer density is $4/5$ its close-packed value, and the field strength $EmR/p^2 = 3$. Curve A: for pure attractor points as depicted in Figure 3b; Curve AR: for attractor points correlated with surrounding repeller points; Curve AZ: for attractor points correlated with a random set of points.

a separation $< r$ from an arbitrary point of S_1 , summed over all points of S_1 and divided by M^2 . If S_1 and S_2 are identical, the slope of $\ln C(r)$ as a function of $\ln r$ yields the correlation dimension D_2 for this set. The curve labelled AA in Figure 6 refers to this case, where $S_1 = S_2$ is the attractor depicted in Figure 3b. From its slope we find $D_2 = 1.69$ for the attractor (and repellor) which — as theoretically required — is less than D_1 . AR in Figure 6 refers to the case that S_1 is associated with the attractor and S_2 with the repellor. Furthermore, in the curve with label AZ S_1 is the attractor, but S_2 is a set of points randomly sprinkled onto the phase space. It is surprising that the slope of AR is equal to two, also the result for the random case AZ. This indicates that there is very little correlation between attractor and repellor points.

We have analyzed the complex dynamical features of this nonequilibrium steady-state model by constructing a two-dimensional Poincaré map, from one collision of the wanderer particle to the next. But the actual generation of this map is algorithmically rather complicated. Not only are collisions possible with nearest neighbors and second-nearest neighbors of scatterers in the lattice, also higher-neighbor collisions are possible. To avoid this complexity we have sought out the simplest possible two-dimensional map which has the features of time-reversibility, ergodicity (and as a consequence the absence of stable fixed points), and dissipation.

This map is described in the following section.

3. TIME-REVERSIBLE, DISSIPATIVE MAPS

A map \mathbf{M} is said to be time reversible if it satisfies the identity

$$(x, y) = \mathbf{TMTM}(x, y). \quad (13)$$

\mathbf{T} represents velocity reversal (changing the signs of any velocities or friction coefficients). Here we interpret (x, y) as a typical (coordinate, momentum) pair of variables and require that time reversal only changes the sign of y :

$$(x, -y) = \mathbf{T}(x, y). \quad (14)$$

Two applications of the time-reversal operator yield the identity $\mathbf{TT} = \mathbf{I}$.

Evidently the maps corresponding to area-preserving shears, parallel to the x or y axes,

$$\mathbf{X}: (x, y) \rightarrow (x + y, y), \quad (15)$$

$$\mathbf{Y}: (x, y) \rightarrow (x, x + y), \quad (16)$$

are time reversible. For \mathbf{X} the sequence of operations gives:

$$\mathbf{TXTX}(x, +y) = \mathbf{TXT}(x + y, +y) = \mathbf{TX}(x + y, -y) = (x, +y).$$

\mathbf{XY} , the well-known “Cat Map,” is not reversible. But symmetric combinations of \mathbf{X} and \mathbf{Y} are area preserving and time reversible.²¹

Because dissipation corresponds to the shrinking of phase-space volume associated with heat loss, any model with properties analogous to the Galton Board must allow area changes. The simplest such map is a “reflection” about a mirror located at $x = m$ (Ref. 21). For example,

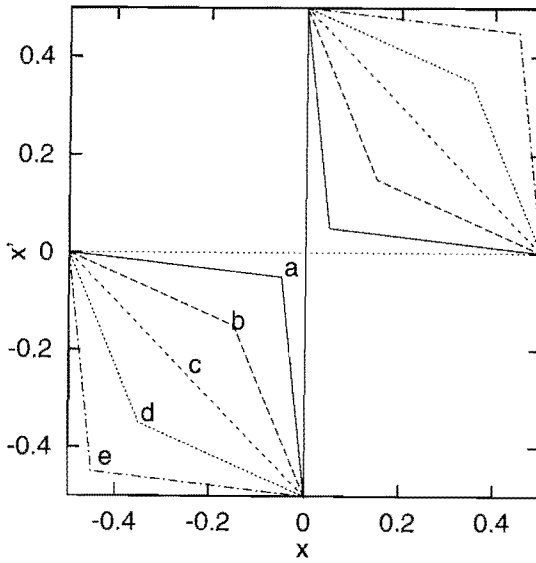


Figure 7. Reflection map \mathbf{P} defined in Section 3 for various values of m : (a) 0.05; (b) 0.15; (c) 0.25, equilibrium; (d) 0.35; (e) 0.45.

if we wished to map the regions $(0 < x < m)$ and $(m < x < 1/2)$ into each other, we can define the reflection operation \mathbf{R}_x according to

$$\begin{aligned} x' &= m + [(2m - 1)/2m](x - m) & \text{for } x < m \\ x' &= m + [2m/(2m - 1)](x - m), & \text{for } x > m, \end{aligned} \quad (17)$$

where negative x are treated analogously. This is a piecewise linear map for $-1/2 < x < 1/2$ with two values of the slope. It is depicted in Figure 7 for various values of m , $0 < m < 1/2$. The case $m = 1/4$ corresponds to the area-preserving equilibrium case.

If we apply simultaneous reflections in both the x and y directions, $\mathbf{P} = \mathbf{R}_x \mathbf{R}_y = \mathbf{R}_y \mathbf{R}_x$, we can generate a time-symmetric map \mathbf{XYPYX} on the unit square $-1/2 < x < 1/2, -1/2 < y < 1/2$ with periodic boundary conditions, which has expanding and contracting regions as required. This map turns out to be ergodic, without stable fixed points, and to show the same type of topological behavior exhibited by the driven Lorentz Gas (Galton Board) example of Section 2, the formation of attractor — repeller pairs with a reduced information dimension.²¹ Attractors generated with this map are shown in Figures 8 for various values of the control parameter m . The information dimension is less than two. Just as in the Galton Board case,¹⁷ the dimensionality loss is quadratic in the deviation from equilibrium, here the deviation of m from the area-preserving value, $1/4$.

Vance has recently pointed out that also a time-reversible variant \mathbf{B} of the familiar baker transformation may be constructed.²⁸ It involves a rotation of the unit square by $\pi/4$ as shown in Figure 9. A cut, parallel to, and closest to, the upper left edge results in two rectangles. Application of \mathbf{B} maps the smaller upper rectangle — without rotation — into the smaller darker region shown at the bottom of the third image of the upper row. The mappings of the two rectangles both include an unstable direction in which the length is stretched and a perpendicular stable direction in which lengths are compressed. As before, \mathbf{T} denotes velocity-reversal (in y -direction). Starting from a uniform distribution of points shown in the second

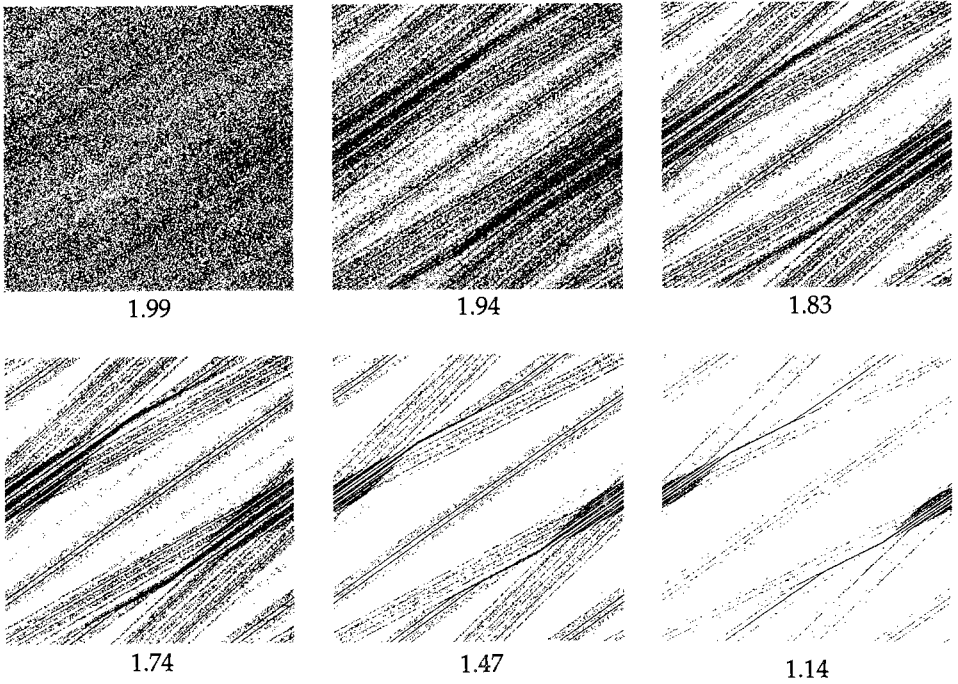


Figure 8. Various attractors generated by the map \mathbf{XYPYX} defined in Section 3. The values for the information dimension D_1 are indicated by the labels. With decreasing D_1 the corresponding values for $\Delta m \equiv m - 0.25$ increase according to 0.01, 0.05, $1/12$, 0.10, 0.15, and 0.17.

square of the upper row in Figure 9, 30 applications of \mathbf{B} generate the attractor (top right) which is transformed into the repeller (bottom right) by \mathbf{T} . 60 subsequent applications of \mathbf{B} lead back to the attractor as displayed in the bottom left frame. Both in the forward and backward direction the trajectory leads from the repeller to the attractor, a clear indication of macroscopic irreversibility.

4. LOSCHMIDT'S PARADOX IN NEW CLOTHES

What have we learned from our small-scale study of irreversible behavior in reversible systems? We have constructed two simple models, one continuous and one discrete, with properties typical of much more complicated macroscopic systems:

1. *Time reversibility* of the equations of motion: The notion of time reversibility we have employed in this work is best discussed in terms of equation (13), if \mathbf{M} is interpreted as a general propagator moving the state of the system *forward* in time. Application of the time-reversal operation \mathbf{T} at time t changes the sign of all momentum components and thermostat variables. If one continues to solve the equations of motion forward in time (for $\tau + t, t > 0$), the trajectory is retraced in configuration space.

In the context of Hamiltonian systems this concept of reversibility is referred to as “S-reversibility”²⁹ (and the velocity-inversion operator \mathbf{T} defined in (14) is denoted

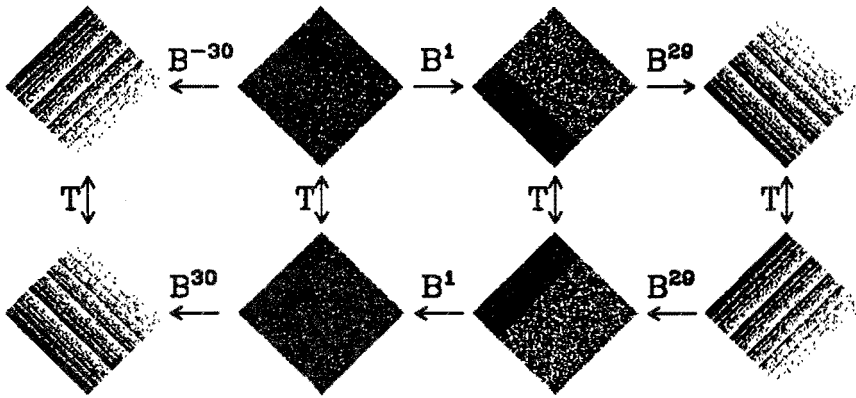


Figure 9. Time-reversible baker transformation B . In the forward direction (upper row) 60 applications of this map lead from the repeller (top left) to the attractor (top right). After time reversal (lower row) the trajectory leads from the repeller (bottom right) to the attractor (bottom left).

by S . There are, however, a number of other concepts of reversibility which are not equivalent.^{29, 30}

2. *Ergodicity*: all accessible phase-space states eventually recur. There are no stable fixed points.
3. *Macroscopic irreversibility*: To relate this concept with the previous ones one has to consider (infinitely) long trajectories in phase space, starting from selected initial conditions. The phase flow always leads from the repeller to the attractor regardless of the direction of time, a manifestation of macroscopic irreversibility.
4. *Dissipation*: The work supplied by the external perturbation is dissipated into heat and extracted by the thermostat with a rate \dot{Q} given by (5). This heat transfer is essential and makes volume changes possible in the continuous phase space.

The key to an understanding of these properties is the appearance of a Lyapunov-stable attractor and Lyapunov-unstable repeller in phase space which are transformed into each other by the application of T . From any point on the repeller there is a trajectory leading to points on the attractor regardless of the direction of time. Nevertheless, the system continues to be ergodic and all states of the system remain accessible, even though they are of zero probability relative to equilibrium states. We have the paradoxical situation that both the repeller and the attractor are supported by the whole equilibrium phase space and that these fractal objects are intimately interwoven in phase space.

Thus, Loschmidt's and Zermelo's objections reappear in new clothes. We are confident that by the study of such simple models, time continuous and discrete, as presented on this paper we will approach closer to an understanding of macroscopic irreversibility, honoring the memories of Boltzmann, Loschmidt, Poincaré, and Zermelo.

ACKNOWLEDGMENTS

We thank Bill Vance for a number of fruitful discussions. The authors gratefully acknowledge the financial support from the *Fonds zur Förderung der wissenschaftlichen Forschung*,

Grant P09677, and the generous allocation of computer resources by the Computer Center of the University of Vienna. Work in Livermore was supported, in part, by the Lawrence Livermore National Laboratory, under the auspices of the United States Department of Energy through Contract W-7405-Eng-48, in part, by a grant from the Agency for Defense Development, Republic of Korea, and, in part, through the Interuniversity Transfer Agreement for the support of O. Kum.

REFERENCES

1. L. Boltzmann, *Vorlesungen über Gastheorie, I. und II. Teil*, Ludwig Boltzmann Gesamtausgabe, Vol. 1, Akad. Druck- und Verlagsanstalt, Graz, 1981.
2. J. Loschmidt, "Über den Zustand des Wärmegleichgewichtes eines Systems von Körpern mit Rücksicht auf die Schwerkraft," *Sitzungsber. Kais. Akad. Wiss. Wien, Mathemat. Naturwiss. Classe*, II. Abt. **73**, 128 (1876).
3. E. Zermelo, "Über einen Satz der Dynamik und die mechanische Wärmetheorie," *Ann. Phys.* **57**, 485 (1896).
4. L. Boltzmann, *Sitzungsber. Kais. Akad. Wiss. Wien, Mathemat. Naturwiss. Classe*, II. Abt. **75**, 67 (1877); English translation: S. G. Brush, *Kinetic Theory, Vol. 2. Irreversible Processes* (Pergamon, Oxford, 1966), p. 188.
5. J. O. Hirschfelder, C. F. Curtiss, and R. B. Bird, *Molecular Theory of Gases and Liquids* (Wiley, New York, 1954).
6. H. A. Posch, H. Narnhofer, and W. Thirring, "Externally perturbed unstable systems," *J. Stat. Phys.* **65**, 555 (1991).
7. W. G. Hoover, "Temperature, least action, and Lagrangian mechanics," *Phys. Lett.* **A 204**, 133 (1995).
8. D. J. Evans, W. G. Hoover, B. H. Failor, B. Moran, and A. J. C. Ladd, "Nonequilibrium molecular dynamics via Gauss's principle of least action," *Phys. Rev.* **A 28**, 1016 (1983).
9. D. J. Evans and G. P. Morriss, *Statistical Mechanics of Nonequilibrium Liquids* (Academic Press, London, 1990).
10. W. G. Hoover, *Computational Statistical Mechanics* (Elsevier, Amsterdam, 1991).
11. B. L. Holian, W. G. Hoover, and H. A. Posch, "Resolution of Loschmidt's paradox: The origin of irreversible behavior in reversible atomistic dynamics," *Phys. Rev. Lett.* **59**, 10 (1987).
12. H. A. Posch, W. G. Hoover, and B. L. Holian, "Time-reversible molecular motion and macroscopic irreversibility," *Ber. Bunsenges. Phys. Chem.* **94**, 250 (1990).
13. J. D. Farmer, E. Ott, and J. A. Yorke, "The dimension of chaotic attractors," *Physica* **D 7**, 153 (1983).
14. N. I. Chernov, G. L. Eyink, J. L. Lebowitz, and Ya. G. Sinai, "Steady-state electrical conduction in the periodic Lorentz gas," *Comm. Math. Phys.* **154**, 569 (1993).
15. W. N. Vance, "Unstable periodic orbits and transport properties of nonequilibrium steady states," *Phys. Rev. Lett.* **69**, 1356 (1992).
16. W. G. Hoover and B. Moran, "Phase-space singularities in atomistic planar diffusive flow," *Phys. Rev.* **A 40**, 5319 (1989).
17. B. Moran, W. G. Hoover, and S. Bestiale, "Diffusion in a periodic Lorentz gas," *J. Stat. Phys.* **48**, 709 (1987).
18. N. I. Chernov, G. L. Eyink, J. L. Lebowitz, and Ya. G. Sinai, "Derivation of Ohm's law in a deterministic mechanical model," *Phys. Rev. Lett.* **70**, 2209 (1993).
19. Ch. Dellago, L. Glatz, and H. A. Posch, "Lyapunov spectrum of the driven Lorentz gas," *Phys. Rev.* **E 52**, 4817 (1995); Ch. Dellago and H. A. Posch, "Lyapunov spectrum and the conjugate pairing rule for a thermostated random Lorentz gas: Numerical simulations," *Phys. Rev. Lett.* **78**, 211 (1997).
20. Ch. Dellago, H. A. Posch, and W. G. Hoover, "Lyapunov instability in a system of hard disks in equilibrium and nonequilibrium steady states," *Phys. Rev.* **E 53**, 1485 (1996); "Kolmogorov-Sinai entropy and Lyapunov spectra of a hard-sphere gas," *Physica* **A 240**, 68 (1997).
21. W. G. Hoover, O. Kum, and H. A. Posch, "Time-reversible dissipative ergodic maps," *Phys. Rev.* **E 53**, 2123 (1996).
22. J. Machta and R. Zwanzig, "Diffusion in a periodic Lorentz gas," *Phys. Rev. Lett.* **50**, 1959 (1983).
23. T. C. Halsey, M. H. Jensen, L. P. Kadanoff, I. Procaccia, and B. I. Shraiman, "Fractal measures and their singularities: The characterization of strange sets," *Phys. Rev.* **A 33**, 1141 (1986).
24. A. B. Chhabra and R. V. Jensen, "Direct determination of the $f(\alpha)$ singularity spectrum," *Phys. Rev. Lett.* **62**, 1327 (1989).
25. J.-P. Eckmann and D. Ruelle, "Ergodic theory of chaos and strange attractors," *Rev. Mod. Phys.* **57**, 617 (1985).
26. H. A. Posch and W. G. Hoover, "Lyapunov instability of dense Lennard-Jones fluids," *Phys. Rev.* **A 38**, 473 (1988).
27. P. Grassberger and I. Procaccia, "Measuring the strangeness of strange attractors," *Physica* **9D**, 189 (1983).
28. W. N. Vance, unpublished.

29. R. Illner and H. Neunzert, "The concept of irreversibility and statistical physics," *Transport Theory and Statistical Physics* **16** (1), 89 (1987).
30. J. A. G. Roberts and G. R. W. Quispel, "Chaos and time-reversal symmetry. Order and chaos in reversible dynamical systems," *Physics Reports* **216**, 63 (1992).